



Effect of Cavities on the Behavior of Piles Under Seismic Loading in Sandy Soils

Mina M. Jameel^{1,*}, and Balqees A. Ahmed²

¹ Department of Civil Engineering, University of Baghdad, Baghdad, Iraq, meena.mohammad188@gmail.com

² Department of Civil Engineering, University of Baghdad, Baghdad, Iraq, balqees.a@coeng.uobaghdad.edu.iq

*Corresponding author: Mina M. Jameel, email meena.mohammad188@gmail.com

Published online: 31 December 2022

Abstract— The effect of cavities on the piles group foundation settlement under the seismic loads in dry sandy soil is investigated throughout this paper. The behavior of soil under a group of piles with cavity formation was represented by finite element program (Plaxis 3D 2020). The study looked at the existence of a single cavity as well as a different numbers of cavities in various locations. This research illustrates the maximum value for total vertical and horizontal displacement for piles under dynamic load El-Centro earthquake with cavity and without cavity. When the cavity was positioned closed to the tip of the piles, the influence of the (El Centro) earthquake load on the settlement of group of piles with cavity grewed the settlement and the difference in total vertical and horizontal displacement.

Keywords— Seismic loading, group piles, sandy soil, cavity, PLAXIS 3D.

1. Introduction

The behavior of soils is regarded as complicated material, unlike most structural materials, to use the structures built on the soil safely, it has to be dealt with it carefully. The presence of cavities is one of the most well-known problems in soils. When the soils contain cavities, they are named “problematic soils” as cavities create structural deterioration and even death. Cavities can be split into two parts, natural and man-made cavities. Natural cavities result from areas going dry, solids disappearing into limestone, and mostly are gypsum. In sandy soil various sizes of cavities ranged from 0.1 m to 3 m [5].

Khalil and Khattab [1] investigated influence of a cavity on the stability of the foundation was investigated by usage non-linear finite element analysis via the PLAXIS 2D and PLAXIS 3D systems. Numerous variables were considered in the study, Including a single cavity's shape, position, size, and depth under the foundation. On isolated square, round, and strip footings, the influence of the factors on the stress distribution and settlement has been investigated. The results indicated for cavity sections that

was selected (Square, Loaf, Circular, Ellipse1, and Ellipse2), the cavity's volume and shape affect the underfoot concentration of the settlement and stress. When a cavity was placed on vertical depth less than 2 times a strip foundation's width or 1.5 times (diameter or width) of isolated (circular or square) foundations, the effect occurs. Additionally, the study demonstrated a significant increase in settlement values and stress concentrations at a depth beneath the footing referred to as the critical depth. Additionally, it was discovered that a zone called the critical zone exists beneath the footing (zone of the failure plane and radial shear). If a cavity forms within this zone, it will have a significant impact. Settlement was significant for cavities lying beneath the footing in this zone.

Al-Recaby[6] investigated the impact of pile group foundation using PLAXIS 3D 2013. It was described the basic finite element method formulation and a verification problem was analyzed from the experimental work. It was examined a full-scale pile group problem under the effect of the real earthquake motion. It was concluded that a good congruence of outcomes from the finite element method

and measured responses from the physical model. It was found the earthquake acceleration greater than the acceleration on soil bed and foundation cap. a results showed that in dry and saturated soils, the maximum horizontal and vertical displacement of the pile cap rises with increasing earthquake amplitude.

AlSheakayree [10] studied the dynamic effect of pile installation in sand on nearby structures by utilizing PLAXIS 3D finite element program. Vibrations may occur either naturally or manmade. on urban areas, a vibration generates cause of pile driving, vehicle movement, heavy machinery or train travel. Earthquakes is natural source of vibrations on subsoil. He calculated influence of vibrations with dynamic analysis at frequency of dynamic load was higher than natural frequency of medium. He calculated low frequency vibrations with a pseudo-static analysis. inertia of subsoil and time dependence of load was considered on modeling dynamic response of a soil structure. It was found that the quality of the finite element model (PLAXIS software) significantly improved by taking into account the friction between pile and soil, considering non-linear behavior of soils, and defining an artificial boundary that minimizes reflection of the waves in the far field.

2. Seismic Waves

When two enormous solid pieces of hard stuff move against each other during an earthquake, elastic waves are generated. This separation of two large solid materials is known as a 'fault'. From the concentrate, seismic 'elastic' waves are generated via the body at all locations. If a solid body's equilibrium, such as the earth, is troubled as an outcome of error movement caused by an earthquake. Earthquakes radiate waves at durations ranging from 10 seconds to some minutes. [11].

2.1 Types of Seismic Waves

Seismic waves can be divided into three main types, P waves, S waves and surface waves as shown in **Figure 1**. P and S waves sometimes called body waves. P waves called primary waves or pressure waves, which travels through the earth at the greatest velocity. As it moves into the air, it take the form of sound waves. It travels by the air at the sound speed (330 m/s) and 5000 m/s in granite. It is the first waves recorded during an earthquake by a seismograph because its high speed.

S waves called Secondary waves, shaking waves or shear waves, are slower-moving transverse waves than P waves. Particle motion in this case is perpendicular to the direction of wave propagation.

Surface waves generating when the earthquake's source is near to the surface of the earth, and it is similar in nature to water waves that transmitted under the earth's surface.

It is slower than S waves; it considered the most destructive type of wave because it is large amplitude.

The two basic types of surface waves are: [9]

- Rayleigh waves, known as ground roll, which travel similar to ripples on the water surface. They noticed this phenomenon during an earthquake in open locations, such as parking lots, where the cars move up and down with the waves.
- Love waves shear the ground horizontally. They are slightly faster than Rayleigh waves in terms of travel time.

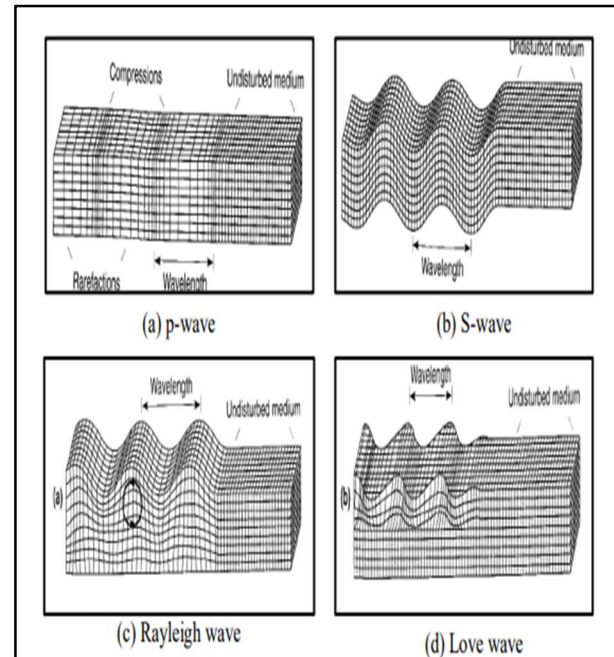


Figure 1: Types of seismic waves [9].

3. Finite Element Modeling

The finite element method has been used in geotechnical problems from 1960, many studies deal with this technique and a lot of books and papers were published on this topic. This method is applicable to the soil which is displaying nonlinear -stress-strain behavior, which considered a noticeable advantage.

3.1 Plaxis program

PLAXIS 3D-2020 has three main modes which are Model construction, Calculation and Output mode (3D-PLAXIS Manual, 2020):

- Model mode: This mode consists the model geometry construction. The properties of material and boundaries of soil layer are set. The element of construction, like piles, walls and beams are positioned and the characteristics of the materials are set. The setting of loads (static or

dynamic) and finally, the mesh is constructed and polished to the convenient level.

- Calculation mode: This mode consists the phase calculation. Various load status and geometries are grouped to simulate an actual building series. Various conditions of groundwater are set, for every step, and construction of elements the activation process have to be set. Excavation process simulated as deactivation of the phase. The calculation type should be a choice (plastic, dynamic, or consolidation). The plastic calculation is applied to solve the deformation process for elastic-plastic in case of drained and undrained soils. The calculation of stresses and deformations for all the nodes until reaching the ultimate serviceability. The results are based on the selected model of calculation. The dynamic calculations applied to predict dynamic excitations such as the excitation of harmonic or earthquake records. In the mode of calculation there is a choice to preselect points of the model interest. When the points are selected before starting the calculation process, the displacement, stress, and pore pressure of the point in any step or time could be perceived in table or graphic curve.

- Output mode: This mode consists displaying the result of a calculation like deformations, Pore-pressures, dynamic displacements and strains for every calculation stage also, the bending moments of construction elements and the shear forces can be calculated.

3.2 Geometry of 3-D model

This study's model has dimensions of (30*60) m and a depth of 20 m. A geometrical arrangement of situation is shown in Figure 2.

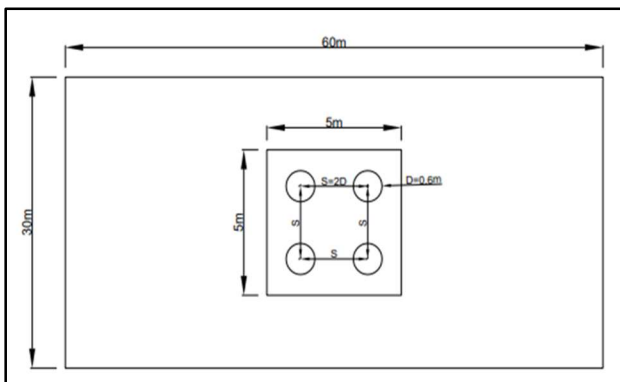


Figure 2: Geometrical arrangements of the situation.

3.2.1 Finite Element Modeling of Pile Group

The model of the pile used in the current research constructed of concrete, as shown in Figure 3. And with the properties given in Table 1.

Table 1: Mechanical properties of concrete pile used.

Diameter (D), m	Length (L), m	No. of piles	Area of the cap, m ²	Thickness of the cap (t), m	Spacing between the piles (center to center) (s), m
0.6	21	4	*5	0.5	1.2

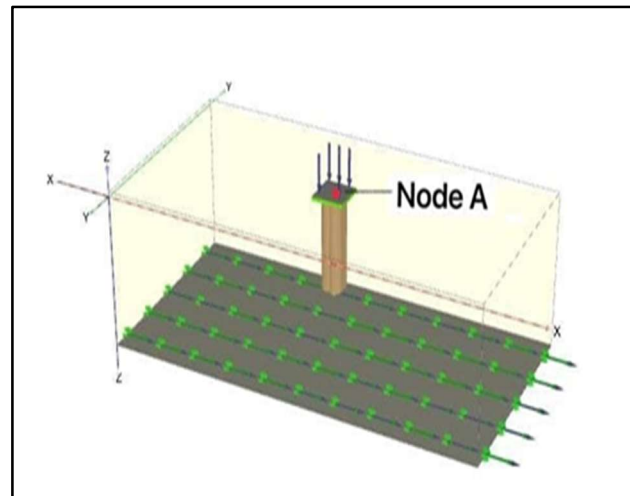


Figure 3: Model pile group.

3.2.2 Finite Element Modeling of a Cavity

In the finite element program (Plaxis 3D foundation 2020), a cavity was modeled via a sphere injunction and by volume element., as shown in Figure 4.

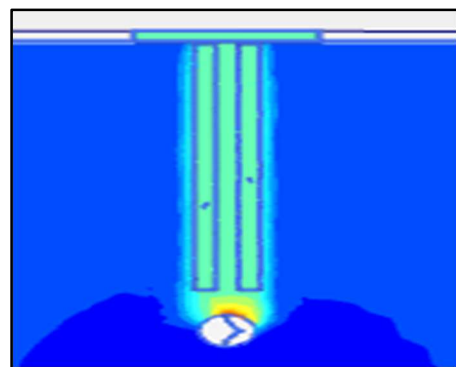


Figure 4: Model of a cavity.

3.2.3 Modeling of Soil

The properties of the soil that used shown in Table 2.

Table 2: Soil properties [4].

Soil properties	Values
Unit weight , γ (kN/m ³)	16
Cohesion, c (kN/m ²)	9
Angle of internal friction, ϕ (°)	19
Modulus of elasticity , E (kN/m ²)	20000
Poisson's ratio ν	0.25

3.2.4 Boundary Condition and Mesh Generation

PLAXIS's standard fixities were utilized to establish dynamic and static boundary conditions. The boundary conditions are mimicked in one or two directions according to the genuine conditions as free or fixed. In dynamic computations, the boundary conditions must be significantly farther apart than in static calculations. Else, the Seismic waves will be mirrored, resulting in model distortion and increased computation time. To circumvent this issue, PLAXIS 3D makes use of the viscous boundary conditions technique (PLAXIS 3D Manual, 2020). To anticipate the reaction of structures subjected to earthquake stimulation by computer simulations, just a small section of the ground must be represented onto a working area and the computation time must be kept to a minimum. Numerous techniques may be used to reduce the amount of time spent computing.

At the bottom of the model, the needed displacement for seismic excitation is defined. Following that, the motion of the seismic input was described in terms of velocity, acceleration over time and displacement. Along the y and z axes, the boundary conditions are fixed, with a constant prescribed displacement along x axis. To eliminate reversals of distinct seismic waves at the model's boundaries, specific conditions are used to attenuate the various seismic waves that propagate through the boundaries. PLAXIS 3D incorporates viscous boundary conditions with dampers that absorb reflected seismic waves, therefore preventing repeated wave transmission at the foundation. The xy-plane is bounded by viscous boundaries.

The boundary conditions for the static analysis stage were utilised similarly to past studies, with the bottom of the mesh fixed against movement in all directions to account for the rock layer's influence, and the left- and right-hand sides of the model permitted to leave only in vertical directions. Furthermore, in the dynamic analysis stage, the viscous boundaries (X max. and X min. as viscose, and the other directions Y, Z as fixed) were considered to reduce the impact of reflection back to the finite element model [7], [3].

The size of mesh was selection as fine model the foundation's reaction, seismic loading was applied based

on the El-Centro earthquake, which had a peak acceleration of 0.35g. The earthquake was simulated using a finite element model with a set acceleration at the bottom (where location of rock layer). [2], [8].

4. RESULTS AND DISCUSSION

4.1 Piles Under Dynamic Load Without Cavity

In this study, El-Centro earthquake is used with a time period of 33 seconds and peak acceleration 0.35. The settlement was calculated under pile cap at node 21012 (A) shown in **Figure 5**.

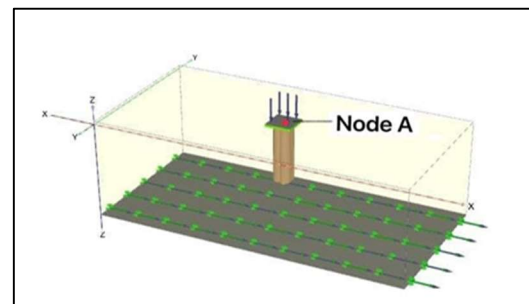


Figure 5: Model pile group.

The results presented in **Figure 6** show that the earthquake load caused the settlement of pile group without cavity with initial loaded 200 kPa. The maximum settlement reaches 5.4 mm under the effect of El-Centro earthquake.

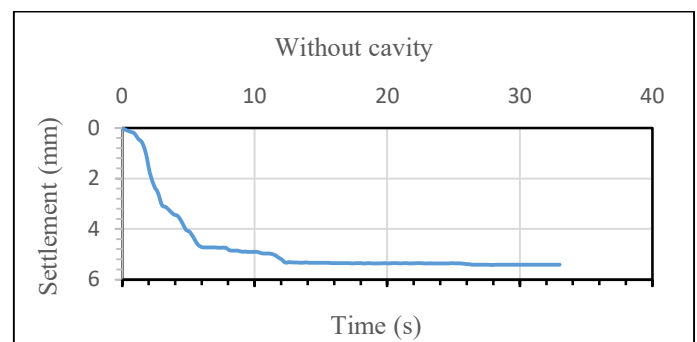


Figure 6: Time-settlement curve of pile group (2x2) in sandy soil without cavity under the effect of El-Centro earthquake.

Figure 7 shows the value of the horizontal displacement (U_x) with time of group of piles (2x2) in sandy soil without cavity under effect of El-Centro earthquake.

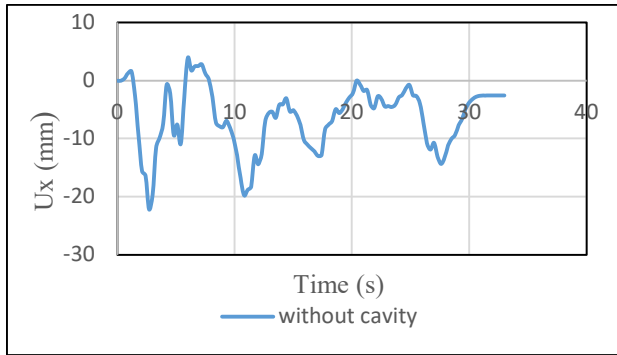


Figure 7: Time – Ux curve of pile group (2x2) in sandy soil without cavity.

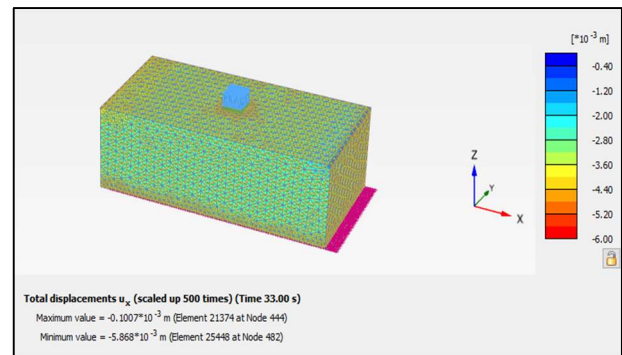


Figure 9: Total horizontal displacement Ux for piles under dynamic load El-Centro earthquake without cavity.

4.1.1 Total displacement Uz and Ux for piles under dynamic load without cavity

Table 3 illustrates the maximum value for total vertical and horizontal displacement for piles under dynamic load El-Centro earthquake without cavity.

Table 3: Total displacement Uz and Ux for piles under dynamic load El-Centro earthquake without cavity.

Model	Max. value for total vertical displacement Uz (mm)	Max. value for total horizontal displacement Ux (mm)
Without cavity	5.461	5.868

Figure 8 shows the value of total vertical displacement Uz for piles under dynamic El-Centro earthquake load without cavity. The max. value was obtained at Node 48991 located under the cap.

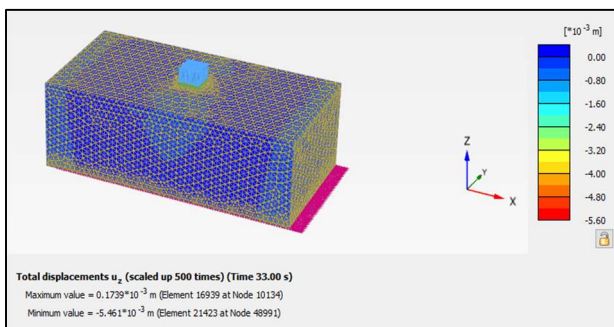


Figure 8: Total vertical displacement Uz for piles under dynamic load El-Centro earthquake without cavity.

Figure 9 shows the value of total horizontal displacement Ux for piles under dynamic El-Centro earthquake load without cavity. The max. value was obtained at Node 482 where located under the cap.

4.2 Piles under dynamic load with cavity in different locations

4.2.1 Piles under dynamic load with a cavity of diameter (d=0.5m) at different vertical depths

Figure 10 shows the influence of alteration the cavity location on the displacement of pile group (2x2) in dry sandy soil with the cavity of diameter (d = 0.5 m) at different vertical depth (Y). While the value of the horizontal distance (X) is fixed under the center of pile group.

There is a rapid increase in settlement when the cavity becomes at close depth (Y=2D) below the pile group base.

The settlement ratio can be defined as follows:

$$\text{Settlement ratio} = (\text{settl. with cavity} / \text{settl. without cavity}) \quad (1)$$

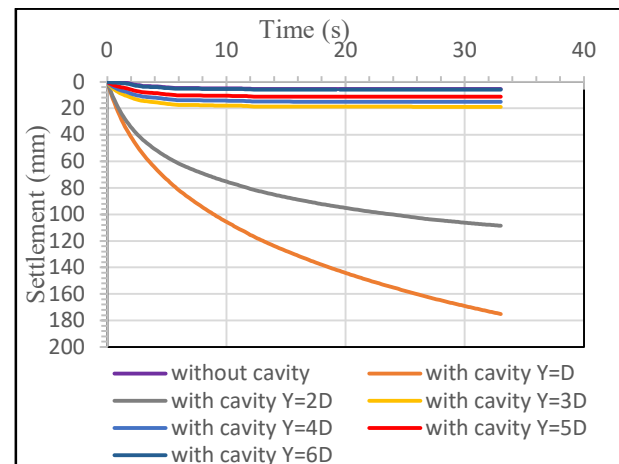


Figure 10: Time-settlement curve of pile group (2x2) in sandy soil with cavity of diameter (d = 0.5 m) at different vertical depths.

Figure 11 illustrates the impact of varying in the vertical distance of the cavity with a diameter of 0.5 m under seismic load in sandy soil with horizontal displacement

(Ux). It is noted that the effect is very small for the Ux and for all vertical locations of the cavity compared to the case without cavity. When the earthquake load is applied, the differences were few because of the high frequency of the El-Centro earthquake, so there is no time for the response to make a difference in the horizontal displacement (Ux).

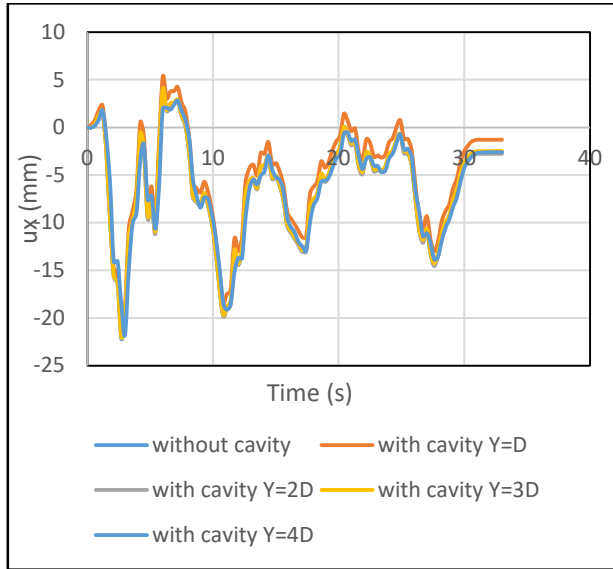


Figure 11: Time – Ux curve of pile group (2x2) in sandy soil with cavity having (d=0.5 m) at different vertical depths.

Table 4 listed the value of settlement ratio for different models and reveals that the presence of cavity vanishes when the cavity is placed at depth Y=6D.

Table 4: Settlement ratio for different vertical locations of cavity (of diameter =0.5 m) below the pile tip.

Model	Settlement ratio, (times)
Y=D=0.6 m	30
Y=2D=1.2 m	20
Y=3D=1.8 m	4
Y=4D=2.4 m	3
Y=5D=3 m	2
Y=6D=3.6 m	1

4.2.2 Total displacement Uz and Ux for piles under dynamic load with a cavity of diameter (d=0.5m) at different vertical depths

Table 5 illustrates the maximum value for total vertical and horizontal displacement for piles under dynamic El-Centro earthquake load with different vertical locations of cavity below the pile group (2x2) in sandy soil with the cavity diameter (d = 0.5 m). The results are obtained from the model completely and it is shown that the highest value for the total vertical and horizontal displacement was increased when the cavity is placed close the edge of the pile.

Table 5: Total displacement Uz and Ux for piles under dynamic load El-Centro earthquake with different vertical locations of cavity below a pile group (2x2) in sandy soil with cavity diameter (d = 0.5 m).

Model	Max. value for total vertical displacement Uz (mm)	Max. value for total horizontal displacement Ux (mm)
Without cavity	5.461	5.868
with cavity Y=D	537.2	428.9
with cavity Y=2D	394.2	166.9
with cavity Y=3D	40.62	36.51
with cavity Y=4D	33.09	16.34
with cavity Y=5D	15.19	8.436
with cavity Y=6D	5.881	6.732

Table 6 shows the difference in total vertical and horizontal displacement for piles under dynamic El-Centro earthquake load with cavity diameter 0.5 m at different vertical depths by using the equations below:

$$\text{Difference in total vertical displacement } U_z = \frac{(U_z \text{ with cavity} - U_z \text{ without cavity})}{U_z \text{ without cavity}} \quad (2)$$

$$\text{Difference in total horizontal displacement } U_x = \frac{(U_x \text{ with cavity} - U_x \text{ without cavity})}{U_x \text{ without cavity}} \quad (3)$$

Table 6: Difference in total displacement Uz and Ux for piles under dynamic El-Centro earthquake load with cavity diameter 0.5 m at different vertical depths.

Model	Difference in total vertical displacement Uz (times)	Difference in total horizontal displacement Ux (times)
with cavity Y=D	97.3	72.0
with cavity Y=2D	71.1	27.4
with cavity Y=3D	6.4	5.2
with cavity Y=4D	5.0	1.7
with cavity Y=5D	1.7	0.43
with cavity Y=6D	0.07	0.14

Figure 12 shows the value of total vertical displacement Uz for piles under dynamic El-Centro earthquake load with cavity diameter 0.5 m and at vertical depth (Y=D). The max. value was obtained at vertical depth (Y=D) at Node 15733 located between the piles and the cavity.

It is illustrated the severe effect of cavity when it is located at shallow depth (Y=D) below the piles under the effect of earthquake.

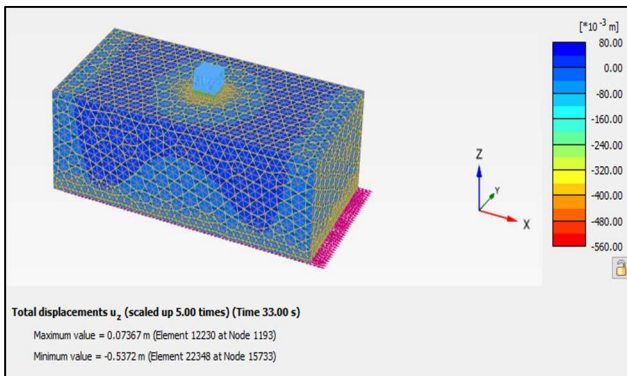


Figure 12: Total vertical displacement Uz for piles under dynamic El-Centro earthquake load with cavity diameter 0.5 m and vertical depth (Y=D).

Figure 13 shows the value of total horizontal displacement Ux for piles under dynamic El-Centro earthquake load with cavity diameter 0.5 m and at vertical depth (Y=D). The max. value was obtained at vertical depth (Y=D) at Node 15753 located between the piles and the cavity.

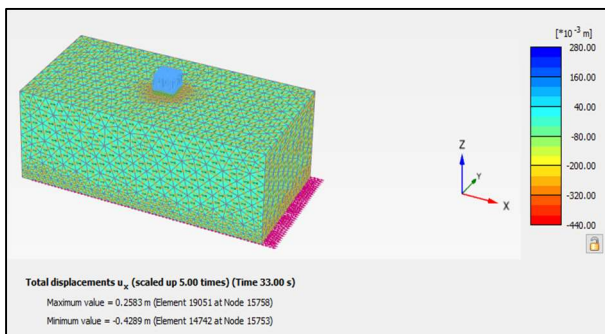


Figure 13: Total horizontal displacement Ux for piles under dynamic El-Centro earthquake load with cavity(Y=D).

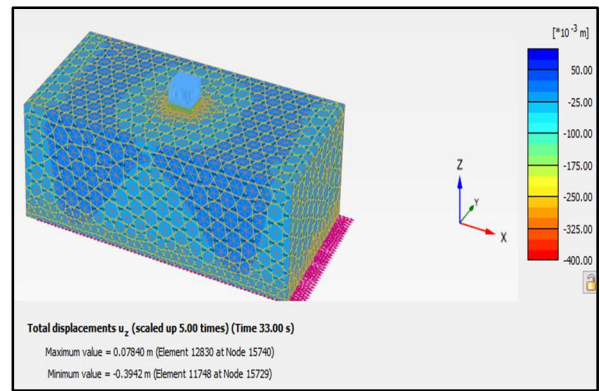


Figure 14: Total displacement Uz for piles under dynamic El-Centro earthquake load with a cavity of diameter (d=0.5 m) at vertical depth (Y=2D).

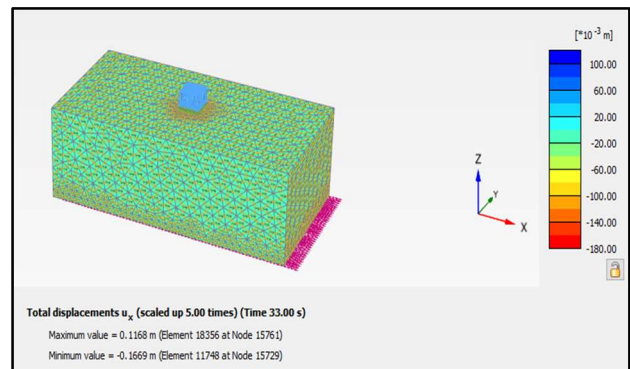


Figure 15: Total displacement Ux for piles under dynamic El-Centro earthquake load with a cavity of diameter (d=0.5 m) at vertical depth (Y=2D).

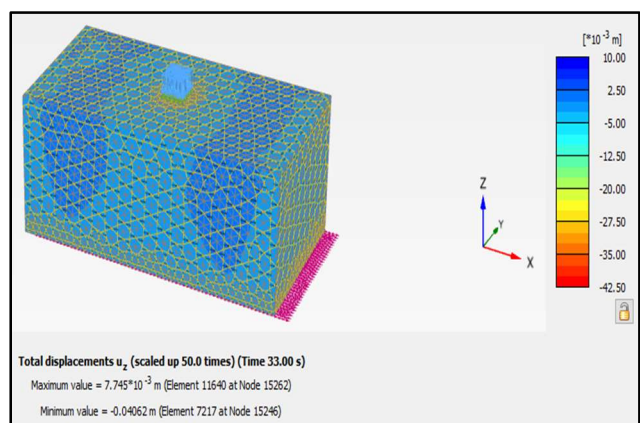


Figure 16: Total displacement Uz for piles under dynamic El-Centro earthquake load with a cavity of diameter (d=0.5 m) at vertical depth (Y=3D).

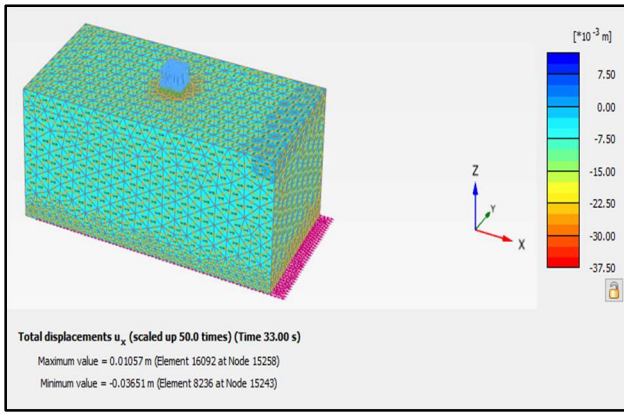


Figure 17: Total displacement U_x for piles under dynamic El-Centro earthquake load with a cavity of diameter ($d=0.5$ m) at vertical depth ($Y=3D$).

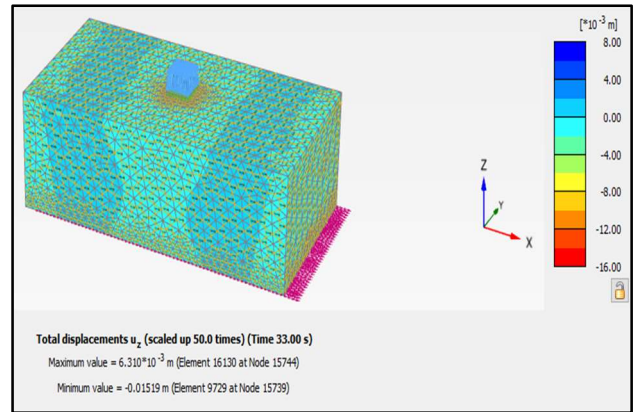


Figure 20: Total displacement U_z for piles under dynamic El-Centro earthquake load with a cavity of diameter ($d=0.5$ m) at vertical depth ($Y=5D$).

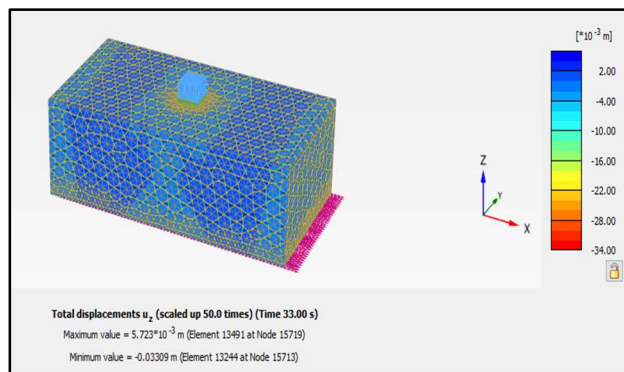


Figure 18: Total displacement U_z for piles under dynamic El-Centro earthquake load with a cavity of diameter ($d=0.5$ m) at vertical depth ($Y=4D$).

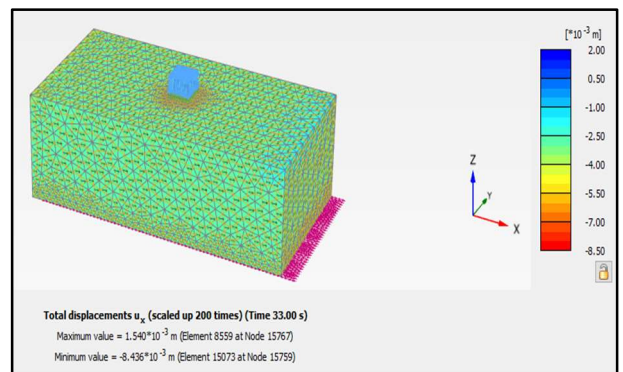


Figure 21: Total displacement U_x for piles under dynamic El-Centro earthquake load with a cavity of diameter ($d=0.5$ m) at vertical depth ($Y=5D$).

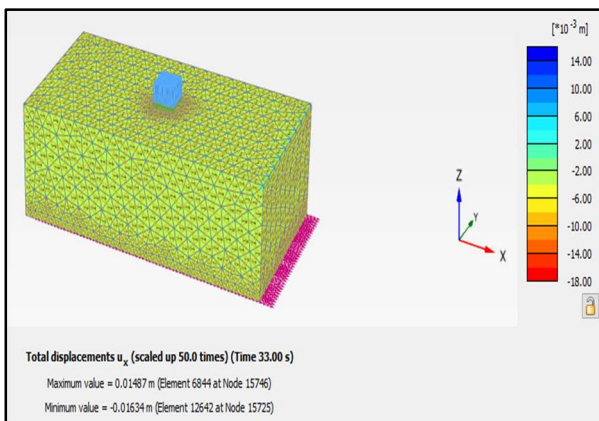


Figure 19: Total displacement U_x for piles under dynamic El-Centro earthquake load with a cavity of diameter ($d=0.5$ m) at vertical depth ($Y=4D$).

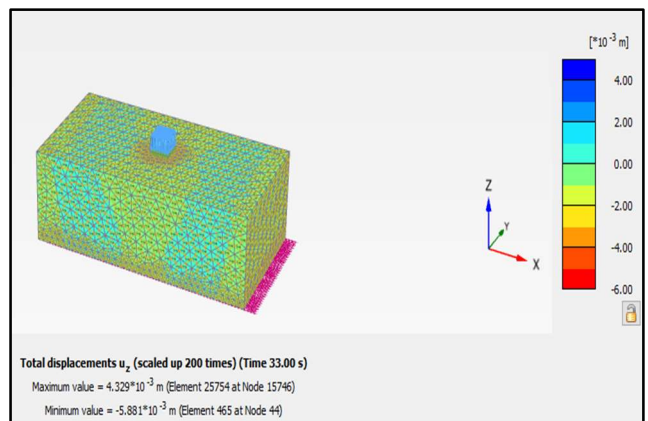


Figure 22: Total displacement U_z for piles under dynamic El-Centro earthquake load with a cavity of diameter ($d=0.5$ m) at vertical depth ($Y=6D$).

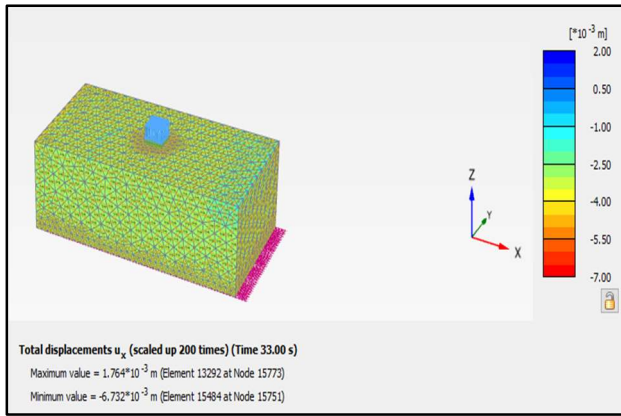


Figure 23: Total displacement U_x for piles under dynamic El-Centro earthquake load with a cavity of diameter ($d=0.5$ m) at vertical depth ($Y=6D$).

4.2.3 Piles under dynamic load with a cavity of diameter ($d=0.5$ m) at different horizontal distances

Figure 24 shows the influence of alteration the cavity location on the displacement of pile group (2×2) in dry sandy soil with the cavity diameter ($d = 0.5$ m) at different horizontal distances (X), while the value of vertical depth (Y) is fixed and equal to D under the effect of (El-Centro) earthquake.

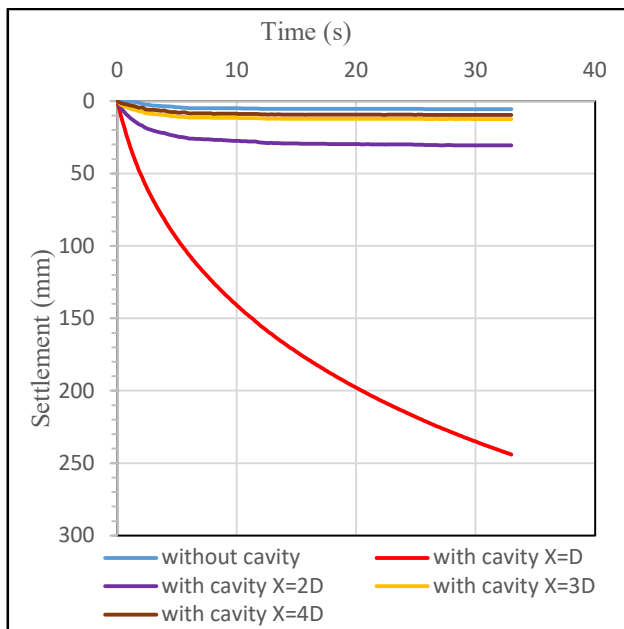


Figure 24: Time-settlement curve of pile group (2×2) in sandy soil with cavity of diameter ($d = 0.5$ m) at different vertical depths.

Figure 25 illustrates the impact of varying in the horizontal distance of the cavity with a diameter of 0.5 m

under earthquake load in sandy soil with horizontal displacement (U_x). It is noted that the effect is very small for the U_x and for all horizontal locations of the cavity compared to the case without cavity.

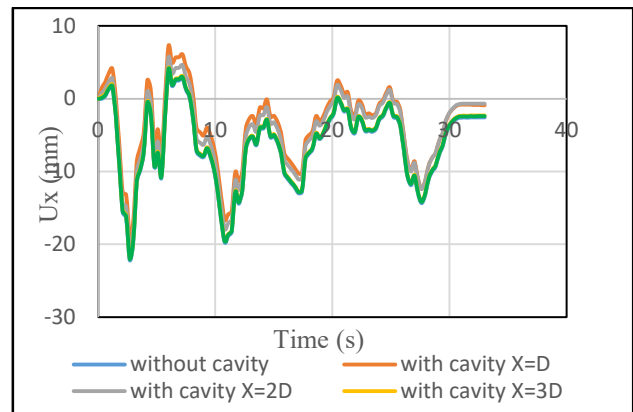


Figure 25: Time – U_x curve of pile group (2×2) in sandy soil with cavity ($d=0.5$ m) at different horizontal distances.

Table 7 listed the value of settlement ratio for different models and reveals that the presence of cavity vanishes when the cavity is placed at distance $X=4D$.

Table 7: Settlement ratio for pile groups with cavity of diameter ($d = 0.5$ m) at different horizontal distances.

Model	Settlement ratio, times
$X=D=0.6$ m	44
$X=2D=1.2$ m	5.3
$X=3D=1.8$ m	2
$X=4D=2.4$ m	1.6

4.2.4 Total displacement U_z and U_x for piles under dynamic load with a cavity of diameter ($d=0.5$ m) at different horizontal distances

Table 8: illustrates the maximum values for total vertical and horizontal displacements for piles under dynamic El-Centro earthquake load with different horizontal distances of cavity below pile group (2×2) in sandy soil. The results showed that the highest value for total vertical and horizontal displacement was when the cavity is placed close the edge of the pile; ($X=D$, $X=2D$, $X=3D$ and $X=4D$)

while the value of vertical depth (Y) is fixed and equal to D.

Table 8: Total displacements U_z and U_x for piles under dynamic El-Centro earthquake load with different horizontal distances of cavity below pile group (2x2) in sandy soil with cavity of diameter ($d = 0.5$ m).

Model	Max. value for total vertical displacement U_z (mm)	Max. value for total horizontal displacement U_x (mm)
without cavity	5.461	5.868
with cavity $X=D$	545.5	606.7
with cavity $X=2D$	61.67	83.32
with cavity $X=3D$	26.46	23.57
with cavity $X=4D$	12.39	17.43

Table 9 Shows the difference in the total vertical and horizontal displacement for piles under dynamic El-Centro earthquake load with cavity diameter 0.5 m at different horizontal distances by using the equations (4.1) and (4.2) mentioned previously.

Table 9: Difference in total displacement U_z and U_x for piles under dynamic El-Centro earthquake load with cavity diameter 0.5 m at different horizontal distances.

Model	Difference in total vertical displacement U_z , (times)	Difference in total horizontal displacement U_x , (times)
with cavity $X=D$	98.8	102.3
with cavity $X=2D$	10.29	13.1
with cavity $X=3D$	3.8	3.0
with cavity $X=4D$	1.2	1.9

Figure 26 indicates that severe horizontal displacement takes place when the cavity is placed at distance ($X=D$) under earthquake loading. The max. value was obtained at horizontal distance ($X=D$) at Node 15727 located between the piles and the cavity.

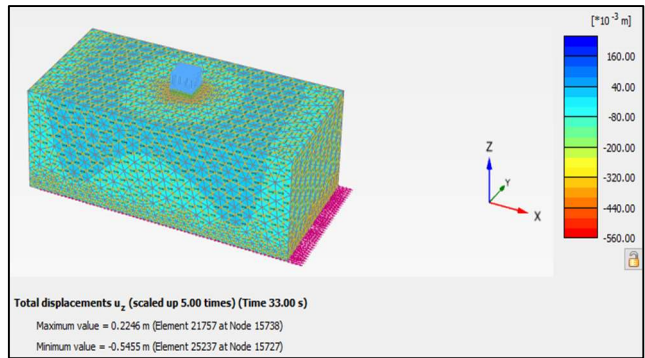


Figure 26: Total vertical displacement U_z for piles under dynamic El-Centro earthquake load with cavity diameter 0.5 m and horizontal distance ($X=D$).

Figure 27 shows the value of total horizontal displacement U_x for piles under dynamic El-Centro earthquake load with cavity diameter 0.5 m and at horizontal distance ($X=D$). The max. value was obtained at horizontal distance ($X=D$) at Node 15730 located between the piles and the cavity.

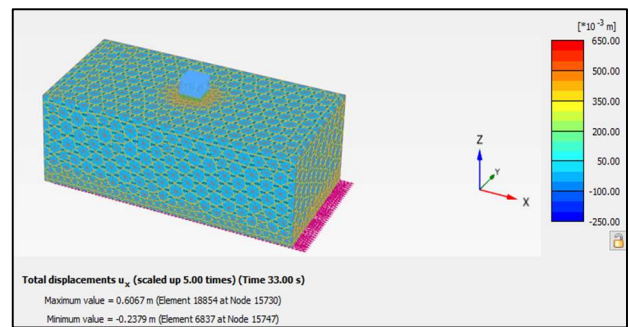


Figure 27: Total horizontal displacement U_x for piles under dynamic El-Centro earthquake load with cavity ($X=D$).

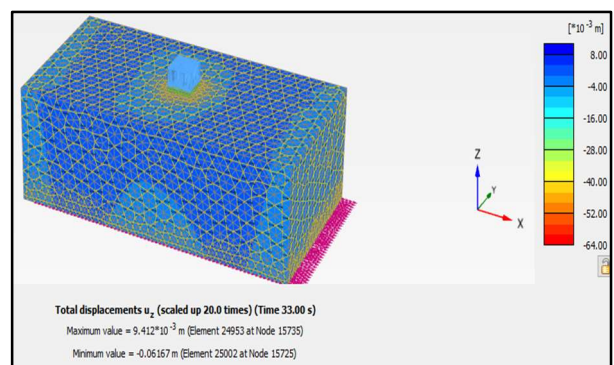


Figure 28: Total displacement U_z for piles under dynamic El-Centro earthquake load with a cavity of diameter ($d=0.5$ m) at horizontal distance ($X=2D$).

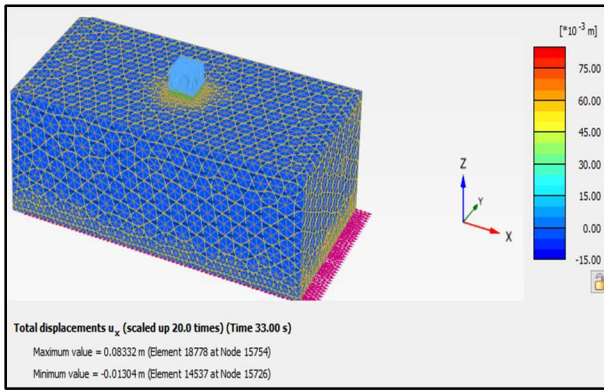


Figure 29: Total displacement U_x for piles under dynamic El-Centro earthquake load with a cavity of diameter ($d=0.5$ m) at horizontal distance ($X=2D$).

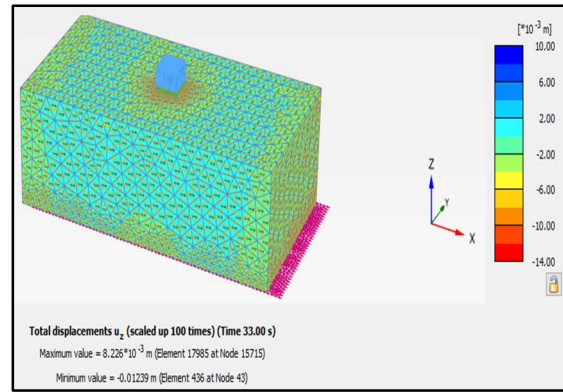


Figure 32: Total displacement U_z for piles under dynamic El-Centro earthquake load with a cavity of diameter ($d=0.5$ m) at horizontal distance ($X=4D$).

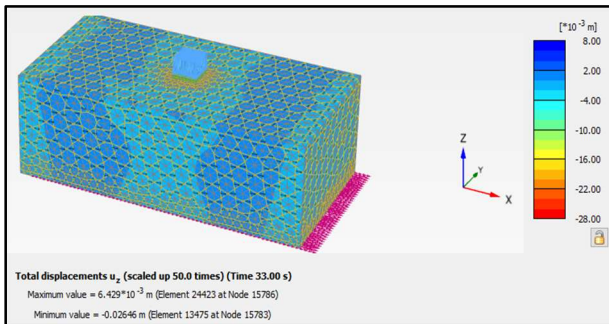


Figure 30: Total displacement U_z for piles under dynamic El-Centro earthquake load with a cavity of diameter ($d=0.5$ m) at horizontal distance ($X=3D$).

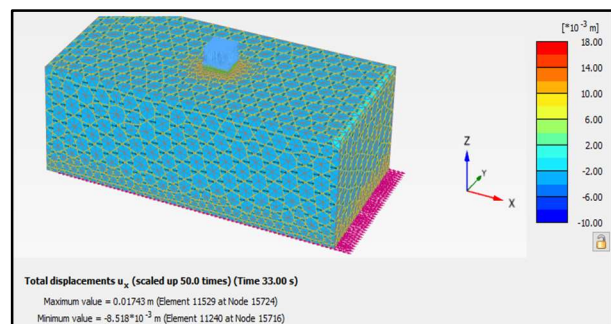


Figure 33: Total displacement U_x for piles under dynamic El-Centro earthquake load with a cavity of diameter ($d=0.5$ m) at horizontal distance ($X=4D$).

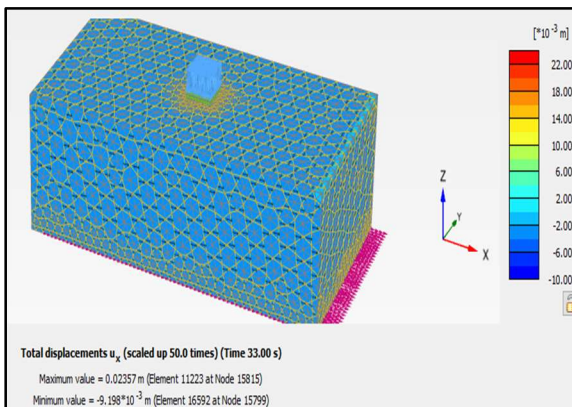


Figure 31: Total displacement U_x for piles under dynamic El-Centro earthquake load with a cavity of diameter ($d=0.5$ m) at horizontal distance ($X=3D$).

4.3 Piles under dynamic load with different number of cavities.

In this paper, the model consists of different number of cavities of diameter ($d=0.5$ m):

- 1- contains 4 cavities as shown in **Figure 34**.
- 2- contains 5 as shown in **Figure 35**.

The results are shown in **Figure 36**.

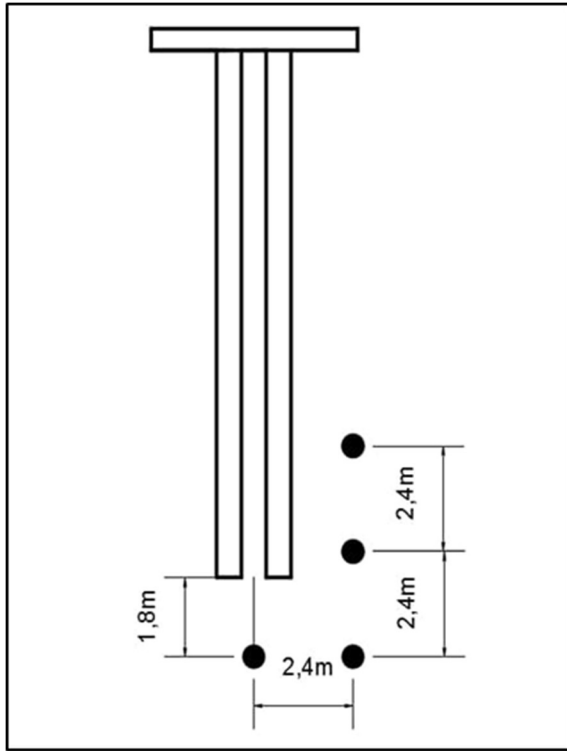


Figure 34: Distribution of the cavities under the effect of dynamic (El-Centro) earthquake load and contains 4 cavities.

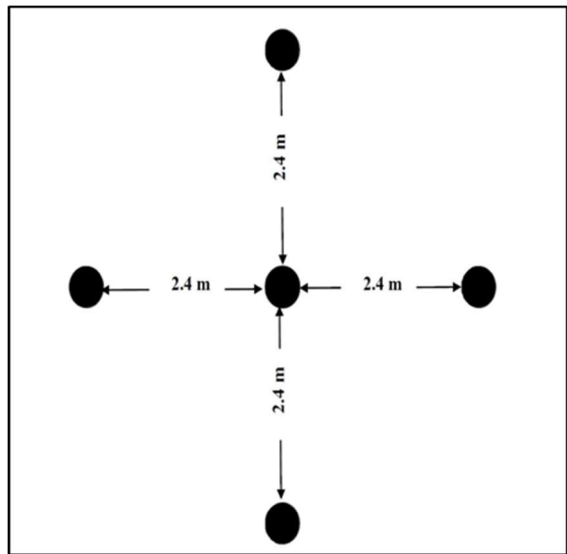


Figure 35: Distribution of the cavities under the effect of dynamic (El-Centro) earthquake load and contains 5 cavities under pile group.

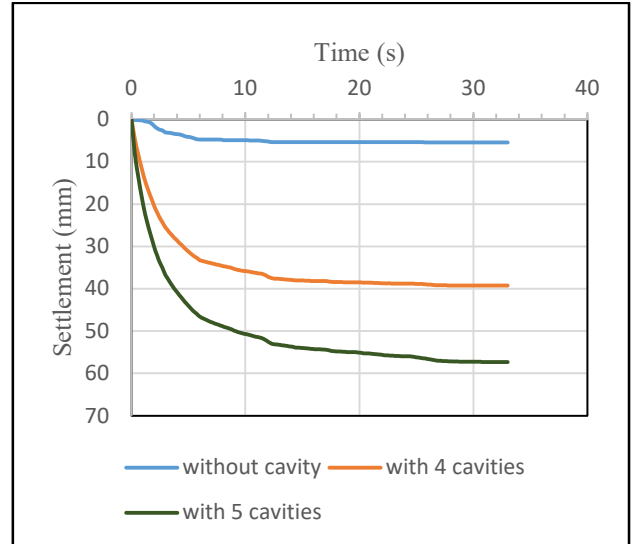


Figure 36: Time-settlement curve of pile group (2x2) in sandy soil with different numbers of cavities of diameter ($d = 0.5$ m) at different locations.

Figure 37 illustrates the impact of varying in the number of cavities with diameter 0.5 m under earthquake load in sandy soil on the horizontal displacement vibration with time. It is noted that there is no effect and the results were completely identical compared to the case without cavity.

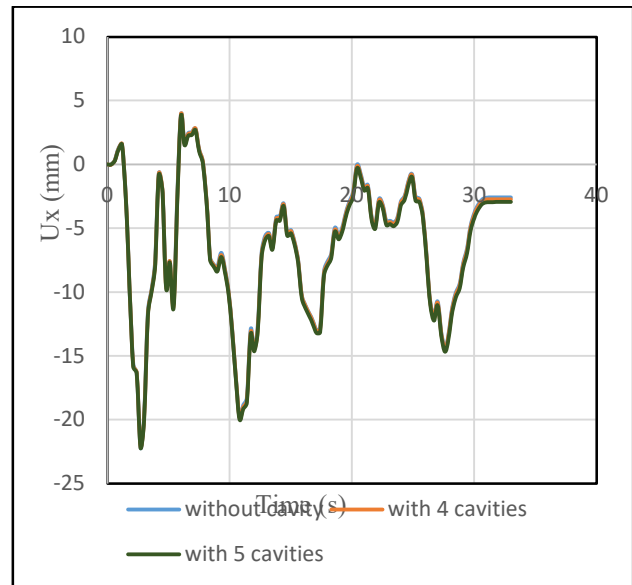


Figure 37: Time-Ux curve of pile group (2x2) in sandy soil with number of cavities of diameter ($d = 0.5$ m) at different locations.

Table 10 Shows that the increase of number of cavities affects the settlement ratio by increasing the amount of it

compared to the case of one cavity at the same distance in the vertical direction $Y = 3D = 1.8$ m.

Table 10: Settlement ratio of different number of cavities.

Model	Settlement ratio, (times)
1 cavity	4
4 cavities	7.2
5 cavities	10.6

4.3.1 Total displacement U_z and U_x for piles under dynamic load with different number of cavities

Table 11 illustrates the maximum value for total vertical and horizontal displacement for piles under dynamic El-Centro earthquake load with different number of cavities below the pile group (2x2) in sandy soil with the cavity diameter ($d = 0.5$ m). The results show that the highest value of the total vertical and horizontal displacement was when the number of cavities was 5 cavities.

Table 11: Total displacements U_z and U_x for piles under dynamic El-Centro earthquake load with different number of cavities below pile group (2x2) in sandy soil with cavity diameter ($d = 0.5$ m).

Model	Max. value for total vertical displacement U_z (mm)	Max. value for total horizontal displacement U_x (mm)
with 4 cavities at $Y=3D$	72.46	66.92
with 5 cavities at $Y=3D$	83.0	84.71

Table 12 shows the difference in total vertical and horizontal displacements for piles under dynamic El-Centro earthquake load with different number of cavities, with cavity diameter ($d=0.5$ m) by using equations (2) and (3) mentioned previously.

Table 12: Difference in total displacement U_z and U_x for Piles under dynamic El-Centro earthquake load with different number of cavities ($d = 0.5$ m).

Model	Difference in total vertical displacement U_z , (times)	Difference in total horizontal displacement U_x , (times)
with 4 cavities at $Y=3D$	12.2	10.4
with 5 cavities at $Y=3D$	14.1	13.4

Figure 38 shows the value of total vertical displacement U_z for piles under dynamic El-Centro earthquake load with 4 cavities ($d=0.5$ m). The max. value was obtained at Node 15845.

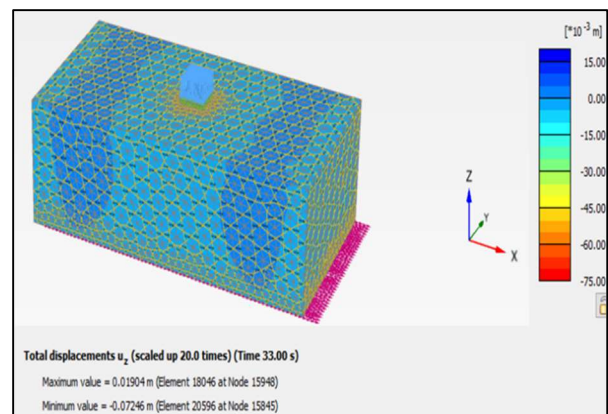


Figure 38: Total vertical displacement U_z for piles under dynamic El-Centro earthquake load with 4 cavities.

Figure 39 shows the value of total horizontal displacement U_x for piles under dynamic El-Centro earthquake load with 4 cavities ($d=0.5$ m).

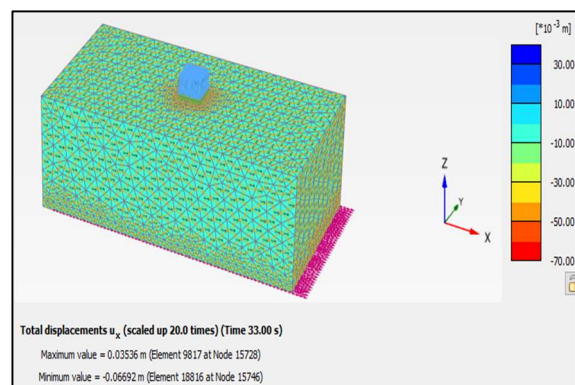


Figure 39: Total horizontal displacement U_x for piles under dynamic El-Centro earthquake load with 4 cavities.

Figure 40 shows the value of total vertical displacement U_z for piles under dynamic El-Centro earthquake load with 5 cavities ($d=0.5$ m). The max. value was obtained at Node 15738.

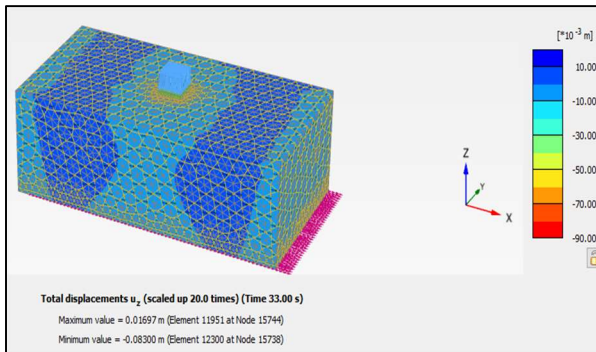


Figure 40: Total vertical displacement U_z for piles under dynamic El-Centro earthquake load with 5 cavities.

Figure 41 shows the value of total horizontal displacement U_x for piles under dynamic El-Centro earthquake load with 5 cavities ($d=0.5$ m). The max. value was obtained at Node 15966.

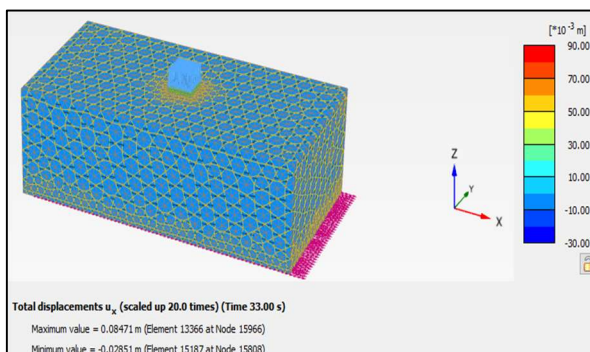


Figure 41: Total horizontal displacement U_x for piles under dynamic El-Centro earthquake load with 5 cavities.

5. CONCLUSIONS

1. When the cavity is positioned towards the tip of the piles, the influence of the dynamic (El-Centro) earthquake load on the settlement of pile groups with cavities led to a rise in settlement.
2. The value of settlement ratio ranges from (30 - 2) times, when the cavity of diameter (0.5 m) placed at vertical depths from ($Y=D$) to ($Y=5D$), and ranges from (44 - 1.6) times when the cavity placed at horizontal distances from ($X=D$) to ($X=4D$).

3. The value of the difference in total vertical displacement (U_z) ranges from (97.3 - 0.07) times, when the cavity of diameter (0.5 m) placed at vertical depths from ($Y=D$) to ($Y=6D$), and the values range from (98.8 - 1.2) times when the cavity placed at horizontal distances from ($X=D$) to ($X=4D$).
4. The value of the difference in total horizontal displacement (U_x) ranges from (72 - 0.14) times, when the cavity of diameter (0.5 m) placed at vertical depths from ($Y=D$) to ($Y=6D$), and the values range from (102.3 - 1.9) times when the cavity placed at horizontal distances from ($X=D$) to ($X=4D$).
5. The rise in the number of cavities has an effect on settlement via raising the amount of settlement extra than one cavity.

6. Acknowledgements

The authors extended their gratitude to the staff of the University of Baghdad's Civil Engineering Department for their assistance and support during the research.

References

- [1] A. A. Khalil and S. A. Khattab, "Effect of cavity on Stress distribution and Settlement under Foundation," *Al-Rafidain Eng. J.*, vol. 17, no. 6, pp. 14–29, 2009.
- [2] A. Kholdebarin, A. Massumi, and M. Davoodi, "Seismic bearing capacity of shallow footings on cement-improved soils," *Earthquakes Struct.*, vol. 10, no. 1, pp. 179–190, 2016.
- [3] D. Mina and D. Forcellini, "Soil–structure interaction assessment of the 23 November 1980 Irpinia-Basilicata earthquake," *Geosciences*, vol. 10, no. 4, p. 152, 2020.
- [4] I. S. Hussein and L. N. Snodi, "Effect of Cavities from Gypsum Dissolution on Bearing Capacity of Soil under Square Footing," in *Key Engineering Materials*, 2020, vol. 857, pp. 221–227.
- [5] K. T. Shlash, M. R. Mahmoud, and L. J. Aziz, "Lateral resistance of a single pile embedded in sand with cavities," *Eng. Tech. J.*, vol. 30, no. 15, pp. 2641–2663, 2012.
- [6] M. K. M. Al-Recaby, "Dynamic Response of Pile Group Model in Sandy Soil to Lateral Excitation." Department of Civil Engineering, University of Technology Baghdad, Iraq, 2016.
- [7] M. Y. Fattah, M. J. Hamoo, and S. H. Dawood, "Dynamic response of a lined tunnel with transmitting boundaries," *Earthquakes Struct.*, vol. 8, no. 1, pp. 275–304, 2015.

- [8] S. Dhar, A. G. Ozcebe, K. Dasgupta, L. Petrini, and R. Paolucci, "Different approaches for numerical modeling of seismic soil-structure interaction: impacts on the seismic response of a simplified reinforced concrete integral bridge," Earthquakes Struct., vol. 17, no. 4, pp. 373–385, 2019.
- [9] S. L. Kramer, Geotechnical earthquake engineering. Pearson Education India, 1996.
- [10] T. K. Q. AlSheakayree, Q. S. M. Shafiq, and A. T. Ibraheem, "The Dynamic Effect of Pile Installation in Sand on Nearby Piles," Al-Nahrain J. Eng. Sci., vol. 20, no. 2, pp. 477–485, 2017.
- [11] T. K. Sen, Fundamentals of seismic loading on structures. John Wiley & Sons, 2009.

Nomenclature

D	Diameter of pile
d	Diameter of cavity
L	Pile length
U _x	Horizontal displacement in x-direction.
U _z	vertical displacement in z-direction.

تأثير التجاويف على سلوك الركائز تحت الحمل الديناميكي في التربة الرملية

ميناء محمد جميل^{1*}، بلقيس عبد الواحد احمد²

¹قسم الهندسة المدنية، جامعة بغداد، بغداد، العراق، Email: meena.mohammad188@gmail.com

²قسم الهندسة المدنية، جامعة بغداد، بغداد، العراق، Email: balqeas.a@coeng.uobaghdad.edu.iq

*الباحث الممثل، ميناء محمد جميل، Email: meena.mohammad188@gmail.com

نشر في: 31 كانون الاول 2022

الخلاصة – تم دراسة تأثير التجاويف على ازاحة مجموعة الركائز تحت الأحمال الزلزالية في التربة الرملية الجافة خلال هذا البحث. تم تمثيل سلوك التربة تحت مجموعة الركائز مع تكوين التجويف ببرنامج العناصر المحدودة (Plaxis 3D 2020). تناولت الدراسة وجود تجويف واحد بالإضافة إلى أعداد مختلفة من التجاويف في مواقع مختلفة. يوضح هذا البحث القيمة القصوى للإزاحة الرأسية والأفقية الكلية للركائز تحت الحمل الديناميكي لزلزال El-Centro مع تجويف وبدون تجويف. عندما تم وضع التجويف بالقرب من طرف الركائز ، أدى تأثير الحمل الزلزالي (El Centro) على ازاحة مجموعة الركائز مع التجويف إلى زيادة الازاحة والفرق في إجمالي الإزاحة الرأسية والأفقية.

الكلمات الرئيسية – التحميل الزلزالي، مجموعة ركائز، التربة الرملية، التجويف ، PLAXIS 3D.